Malik et al., J Geol Geophys 2018, 7:4
DOI: 10.4172/2381-8719.1000445

Journal of Geology & Geophysics
ISSN: 2381-8719

Research Article Open Access

Delineation and Correlation of Lineaments Using Landsat-7 ETM+, DEM and Aeromagnetic Datasets: Basement Complex of Shanono, Northwestern Nigeria

Abdul Malik NF[1]*, Garba I[2], Danbatta UA[2] and Hamza H[2]

[1]*Center for Energy Research and Training, Ahmadu Bello University, Zaria, Nigeria*
[2]*Department of Geology, Ahmadu Bello University, Zaria, Nigeria*

Abstract

An integration of Landsat-7 ETM+, DEM and aeromagnetic datasets was used for basic surficial geologic mapping of the area of study. False colour composite and principle component analysis were derived from three separate bands each with same spatial resolution of 30 m, superimposed over one another. Visible and infra-red waves of the electromagnetic spectrum were sent out to the surface/near surface and the received impulses reveal areas with varying magnetic susceptibilities, displayed on the first vertical derivative map and areas that emitted ranges of heat radiation signatures, displayed on the analytical signal map. Lineaments were conversely extracted from these maps over an area of about 770 km^2. These lineaments represent fractures, faults, discontinuous quartz ridges, river channels, trenches and furrows in field. The eastern major fracture is the Kalangai major fault trending NE-SW. However, a possible presence of a mega fracture structurally controls River Karaduwa with other tributaries trending NW-SE, almost N-S. Part of the area also possesses gold mineralization potentials along the deep seated Kalangai major fault. The lineaments yielded from both datasets were integrated and showed a coincide results of the rate of deformation that most have affected the area to be of brittle/ductile form. The aeromagnetic data exhibits evidence of near surface fractures while the remote sensing data revealed more of surface fractures. Rose plots where inculcated and showed the dominant trend directions of the lineaments to be NE-SW and NW-SE.

Keywords: Lineaments; Kalangai; Landsat-7 ETM+; DEM; First vertical derivative; Analytical signal

Introduction

The Nigerian Basement Complex forms part of the Pan-African terrain which is considered as the southern prolongation of the Central Hoggar [1] and sometimes called Neoproterozoic Trans-Saharan Belt. Black [2] supports the works of Caby [3] and Ajibade and Wright [4] that it was formed during the collision of the West African Craton, Congo Craton and the East Saharan Block. Ball [5] and Wright [6] suggested that the West African Craton subducted beneath the Congo Craton. It consists of older crust of Archean and Palaeoproterozoic ages [7-9]. This gave rise to deformations, metamorphism and extrusion of alkaline to calc-alkaline volcanics [10,11].

According to Oyawoye [12] the Nigerian basement is made up of the following lithologies: Mesozoic-Recent sediments, Younger Granites, Older Granites, undifferentiated Metasediments, Quartzite-quartzite schists, and undifferentiated Basement Complex, which was then modified by Obaje (Figure 1) [13]. The basement rocks was though classified into Migmatite-Gneiss; Metasediments and Metavolcanics; Older Granites; and undeformed acid and basic dykes by Rahaman [14]. It covers major parts of the north, northwest, southwest and parts of north-central, eastern and southern regions. However, about 50% of the Basement Complex is covered by sediments of Cretaceous to Recent age.

Literature Review

The northwestern part of the Nigerian Basement Complex has been studied by several geologists. The geological characteristics of the northwestern region were documented by several authors in terms of their petrology, structural features, hydrogeology, mineralization potentials and geochemical characteristics. The first detailed work carried out in the northwestern part of Nigerian within the Basement Complex was by Truswell and Cope [15]. They studied and discovered impressive structures and contacts between several lithologic units and concluded that the gneissic complex, the schist belts and the Older Granites in the area were formed during a single orogenic event.

The Kalangai fault zone was mapped by Truswell and Cope [15] trending NE-SW for more than 80 km while McCurry [16] and Akinyede [17] mapped it for about 300 km. McCurry [16] has suggested that the Kalangai fault zone is marked by series of breccia zones, ridges, sheared quartzites, mylonites and cataclastic gneiss. These are products of shearing which are evident throughout the fault zone where they occur in form of discrete bodies of mylonites (faulted rocks), thus having protomylonitic or cataclastic texture [18-20]. The zone contains numerous steeply dipping and closely spaced rock pinnacles that strike north-northeast and northeast. It is subvertical with foliation planes trending N40°E and dipping about 38°SE. The rocks are also strongly fractured and highly silicified [21].

Remote sensing (multispectral satellite images and Digital Elevation Model (DEM)) and geophysical techniques (analytical signal and first vertical derivative) were used to delineate associated structural features (fractures, sinistral and dextral faults) with the major fault (Figure 2) which were interpreted to be a trans current fault that cuts across the Kazaure, Kushaka and Malumfashi schist belts and the surrounding parts of the gneissic and granitic complexes in the northwest [16,17,21,22]. The fault extends into the southern part

***Corresponding author:** Abdul Malik NF, Center for Energy Research and Training, Ahmadu Bello University, Zaria, Nigeria, E-mail: nanafatima88@gmail.com

Received January 17, 2018; **Accepted** May 31, 2018; **Published** June 10, 2018

Citation: Abdul Malik NF, Garba I, Danbatta UA, Hamza H (2018) Delineation and Correlation of Lineaments Using Landsat-7 ETM+, DEM and Aeromagnetic Datasets: Basement Complex of Shanono, Northwestern Nigeria. J Geol Geophys 7: 445. doi: 10.4172/2381-8719.1000445

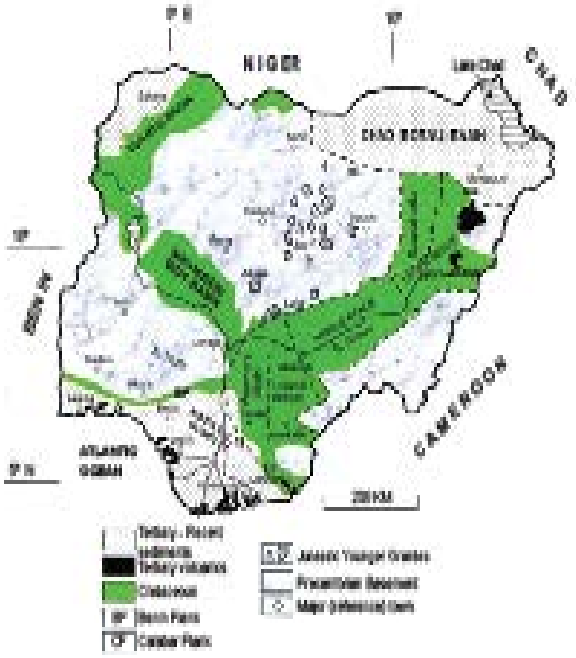

Figure 1: Geologic map of Nigeria showing the major lithologic units.

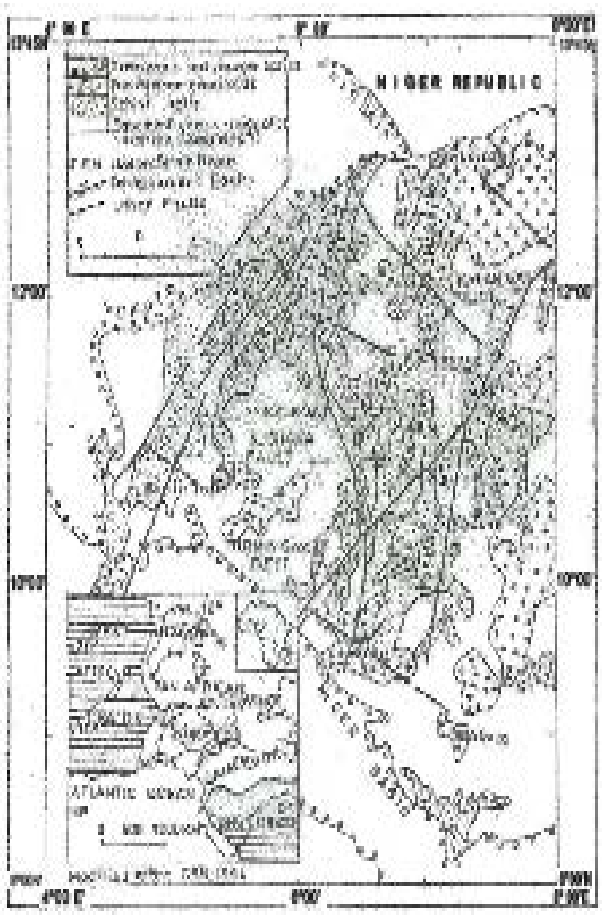

Figure 2: Regional geology and structure of western half of Nigeria showing the major fault systems and minor faults.

of Niger Republic [21,23]. This fault zone has gold mineralization potential. It serves as channel way(s) for the mineralizing solution and as loci of deposition of minerals. This major fault system with the associated structures are of fundamental importance in the selection of zones or target areas for mineral exploration while the contact or shear zones are responsible for the localization of ore deposits [22]. Several geological features associated with the migmatite-gneiss complex and the schist belts in and around the region have been described by Grant, Ajibade, Ball, McCurry, McCurry and Wright, Danbatta, Danbatta and Ike, Danbatta and Garba, Abubakar and Waziri [1,5,10,16,21,22,24-31].

According to McCurry [16], the Kalangai fault system has a total length of about 300 km and a maximum displacement of about 12 km and has fractures which are either indicated by stream channels or as quartz veins. The Kalangai fault has an extensive silicification along its fault trace marked by minor drag folds and the quartz veins [32]. The veins are closely spaced and associated with oblique jointing. Tear faults are also associated with the Kalangai fault system and are formed during late stage of the deformation cycle. These are small dislocations which take up to few kilometers displacement of the main fault. Joint sets are also associated with the Kalangai major fault found on the granites, gneisses and quartzites ridges of the area. They are parallel to the tear faults. Quartzite ridges, mylonites and cataclastic rocks are all identified at the fault zone. The quartzite ridges are discontinuous but its continuance is shown by persistent NE-SW courses of a major river in the area (River Kaduna).

Materials and Methods

The study area is however located in Shanono L.G.A of Kano State and is bounded by latitudes 12°00'00" and 12°15'00"N and longitudes 07°45'00" and 08°00'00"E. The total extent of the study area is 770 km^2 and was mapped at the scale of 1: 50,000, it falls within Sheet 56 Musawa SE. Lithologic and Structural information was best determined from false colour composite in a ratio of 7:4:2 and principle component analysis in a ratio of 3:2:1 (Figure 3). This has shown very useful in structural interpretations according to Bishta. These bands are at specific wavelengths and have a spatial resolution of 30 m (Table 1). This was determined with the aid of ENVI 4.5. However, extraction of lineaments was carried out using ERDAS Imagine 9.2 software. A broader coverage within which the study area falls was used. Six bands of this area were attained from Global Land Cover Facility (GLCF). These images were then exported (as they are already georeferenced) using Global Mapper software to have the exact coordinates of the study area. Bands 7, 4 and 2 were fused to create an image fusion composite in an R, G, and B (Red, Green, and Blue) mode using ENVI software. Before the composites were made, all the Landsat bands were selected, layer stacked and then rearranged accordingly (Figure 4). The bands that were used were highlighted; the first band was the "R", the second was "G" and the third was "B", it was then loaded and saved. However, principal component was selected afterwards, followed by a forward principal component rotation to compute new statistics. Hence, spatial subsets for the bands were selected before loading RGB. The bands selected were 3, 2 and 1 produces less noise. Using this was to further buttress lithologic demarcations and identifies major fractures/faults in the area.

Digital Elevation Model (DEM) was downloaded to study and identify clearly the elevation differences and the lineament features within the study area (Figure 5). This was carried out by searching in the Global Land Cover Facility search for the map area by inserting the latitude and longitude coordinates and SRTM (Shuttle Radar Topographic Mission) was selected, acquired and used for the intended

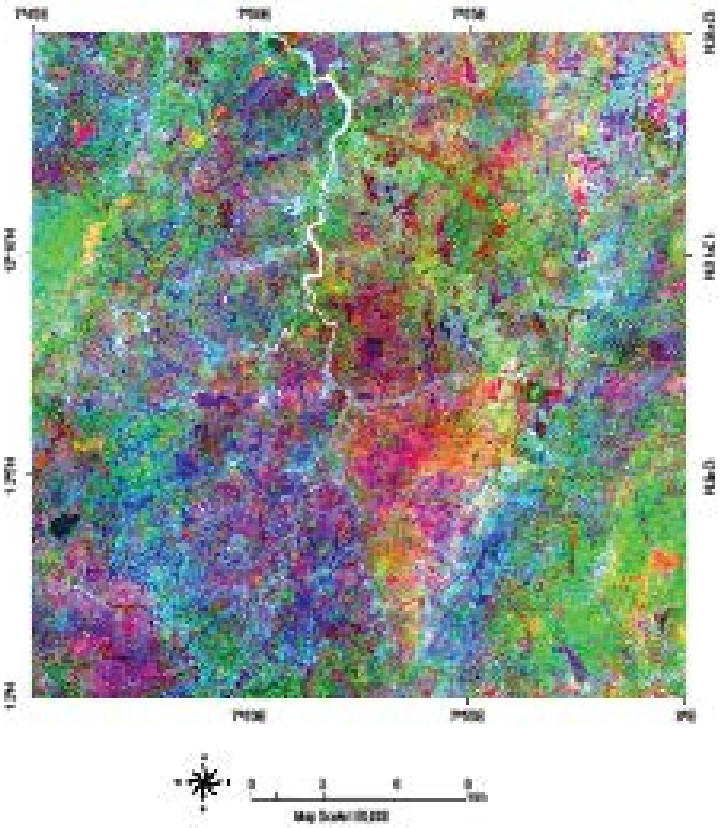

Figure 3: Principal Component Analysis map of study area showing a clearer discrimination between lithologies and two possible major fault zones.

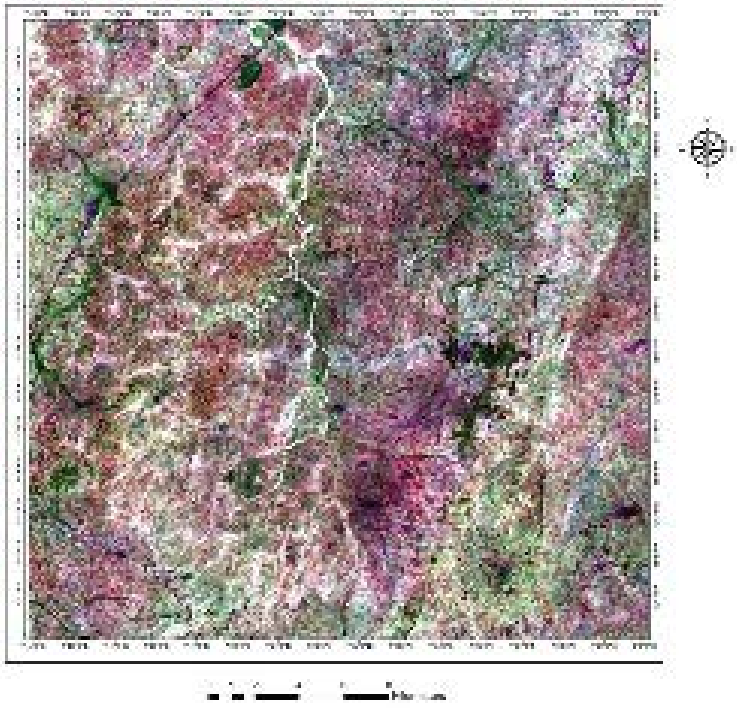

Figure 4: Landsat Enhanced Thematic Mapper image composite of bands 7,4 and 2 discriminating lithologies and zones of structural features (arrows indicating the fault zones).

analysis. This model was next transferred to Global Mapper to extract the bounds of the study area (Figure 6). The colour ramp shader was used to give the varying elevations (slopes) from high to medium to low shaded relief images were created by varying the angle of the sun of the DEM using ERDAS Imagine 9.2 software. They were combined by overlaying them pair by pair to avoid discontinuity this was done until only two combined shaded relief images were left which were saved. It was imported into PCI Geomatica software where the lineaments were generated.

The final shaded relief images that were imported were selected and "RUN" to generate lineaments separately. Their shape files were carried to Arc Map 10.1 where the lineaments were digitized and the lineament density map also generated (Figure 7) buffers were generated round the lineaments in each shaded relief image by reclassifying them into classes. These reclassified maps were then converted into raster image using spatial analyst. Hence, both shaded relief images in raster were then combined using raster calculator which were further digitized.

Aeromagnetic datasets were used to generate major lineaments within the area (Figure 8). Two different datasets were used to generate the First Vertical Derivative image and the Analytic Signal image (Figures 9 and 10). Oasis Montaj software was used to process the data and generate the images. ERDAS Imagine 9.2 and Arc GIS (Arc Map) software were then used to extract and generate the major lineaments. This technique aided to delineate the likely positions and orientations of other possible lineaments that were not identified from Landsat and DEM.

First Vertical Derivative shows areas with high, moderate or low anomalies which include lineaments and delineates zones of different magnetic susceptibility. Analytical signal was also used to delineate structures and lithologies. Different geological features emit radiation at different intensity depending on their shape, size, direction of magnetization and depth. Magnetic anomalies were encountered and recorded across the study area. The results are interpreted alongside with what was identified from the study area. They are otherwise known as "high-resolution data" used for direct detection of geological structures, their trends and provinces.

Results and Discussion

From the false color composite, the water bodies/drainage patterns appears whitish or blue areas, dark blue areas indicating wet/muddy soils, light pink/purple areas as soils/lithologies, greenish areas as vegetation/grasslands. However, the drainages path at the central part of the map appears to be structurally controlled. A dextral sense of shear at the eastern part of the map was observed to be represented by a lighter white tone in the image towards the east.

The blue coloured zones in the PCA represent foliated rocks identified (mylonites towards the east and granite-gneisses towards the west) the greenish, pinkish and reddish regions represent the non-foliated rocks (medium-coarse grained granites and fine grained granites). The PCA confirms two main faults traversing the study area, an eastern dextral strike dip fault trending NE-SW where a shear zone with a dextral sense of shear is situated as well and a western normal dip-slip fault which structurally controls the major river running N-S

Bands	Band Widths (Wave Length) (λ)	Spatial Resolution (Pixel Value)
7	2.06-2.35 μm	30 m
4	0.75-0.90 μm	30 m
3	0.63-0.69 μm	30 m
2	0.525-0.605 μm	30 m
1	0.45-0.515 μm	30 m

Table 1: Band widths (wavelengths) and spatial resolutions of Landsat-7 ETM+ bands used.

Source: NASA.

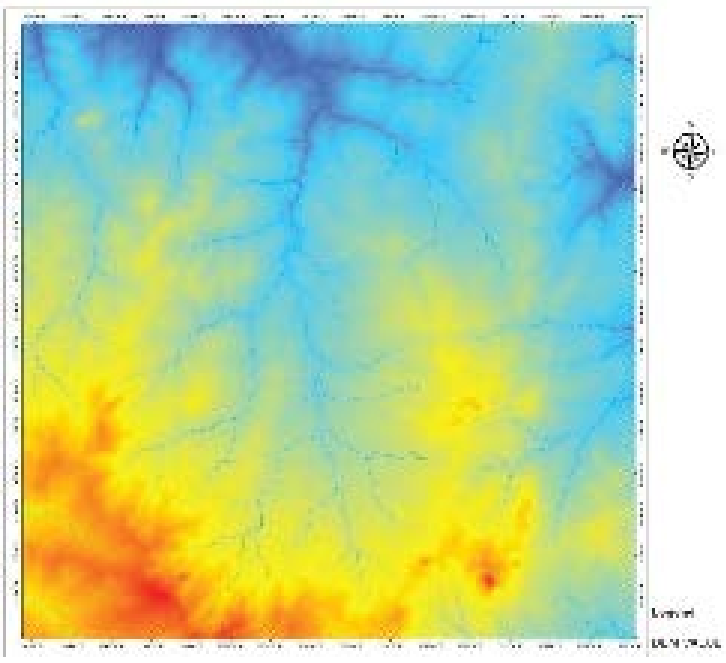

Figure 5: Digital Elevation Model of the study area showing topographic relief from highest to lowest.

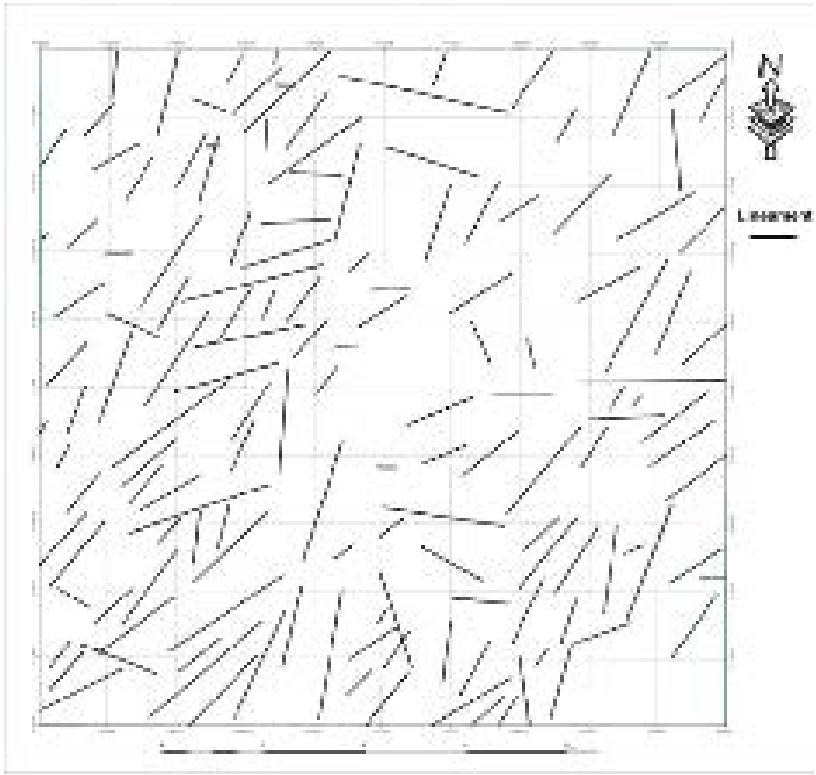

Figure 6: Lineament map produced from Landsat-7 enhanced thematic mapper plus.

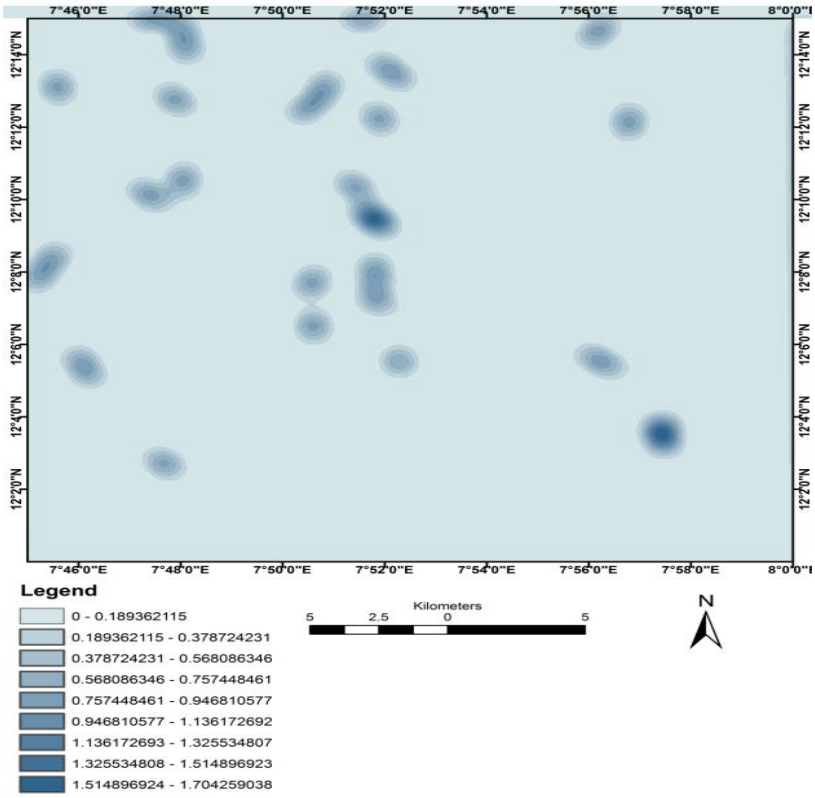

Figure 7: Lineament density map generated from Digital Elevation Model showing zones of lesser and higher concentrations of fractures along the major ones.

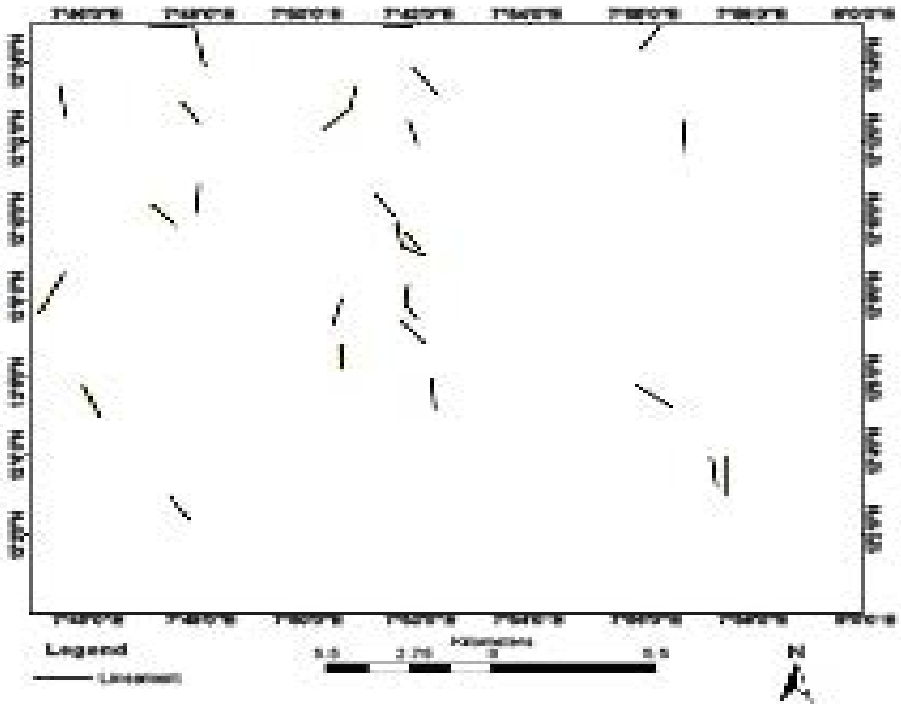

Figure 8: Lineaments extracted from Digital Elevation Model (DEM).

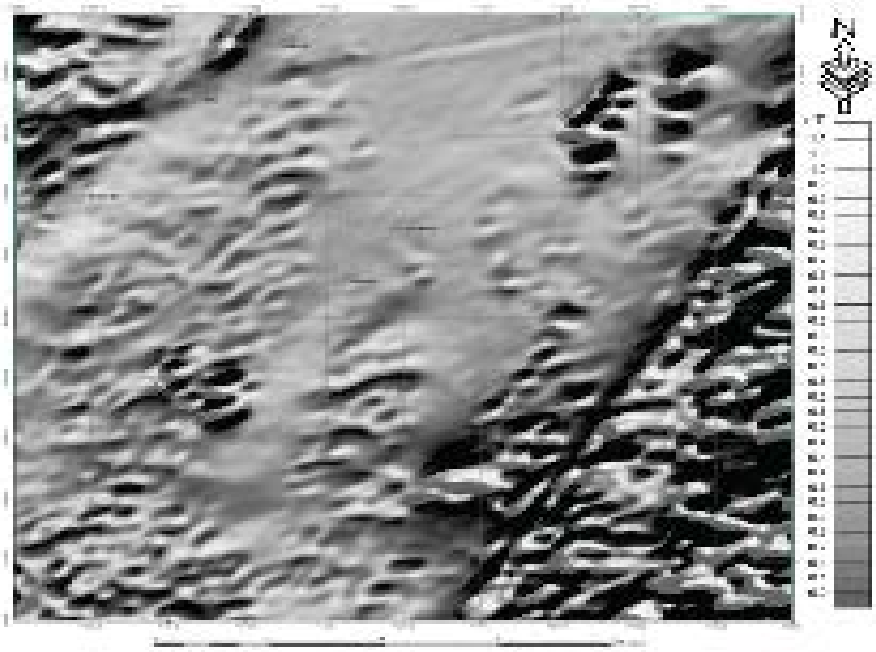

Figure 9: First Vertical Derivative (1VD) image in grey-black scale showing areas of different magnetic susceptibility.

located at the central part. These faults created clear discriminations between the foliated and the non-foliated lithologies. Hence, the gneisses dominating the western area, fine grained granites occupying the central region and the fault/sheared rocks taking up most parts of the eastern region.

About 149 lineaments representing fractures of different degrees, lengths and orientations are shown in. Most of these structures are closely packed and sparse in some areas whilst some indicate truncations. Few of them were observed to be trending in the NW-SE, NNW-SSE and E-W direction while majorly are oriented in the NE-SW direction. The strike lines of the lineaments at the northeastern

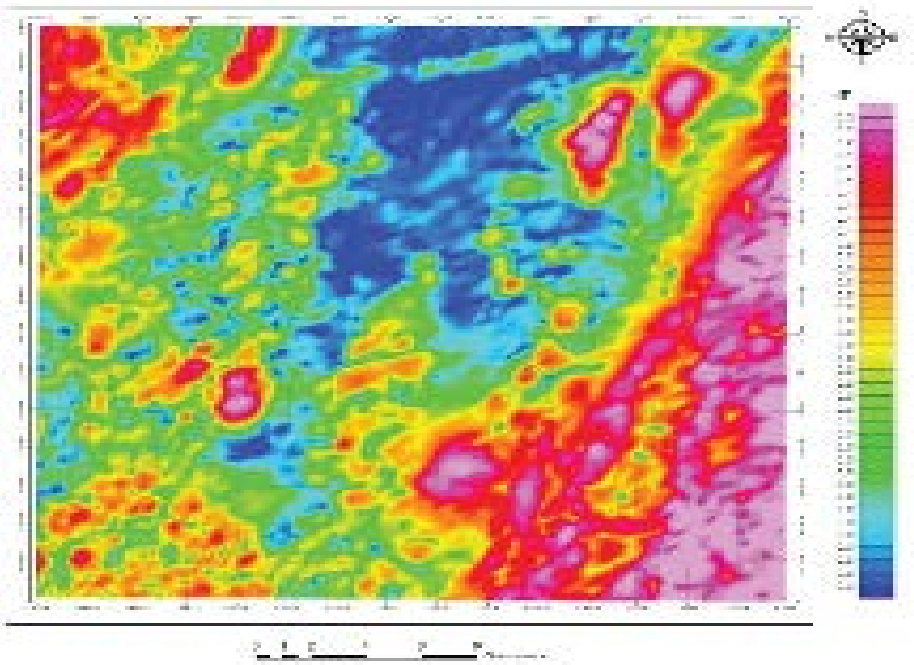

Figure 10: Analytic Signal image with varying strengths of signals of the rock types. The fault/sheared axis in the study area have higher signal.

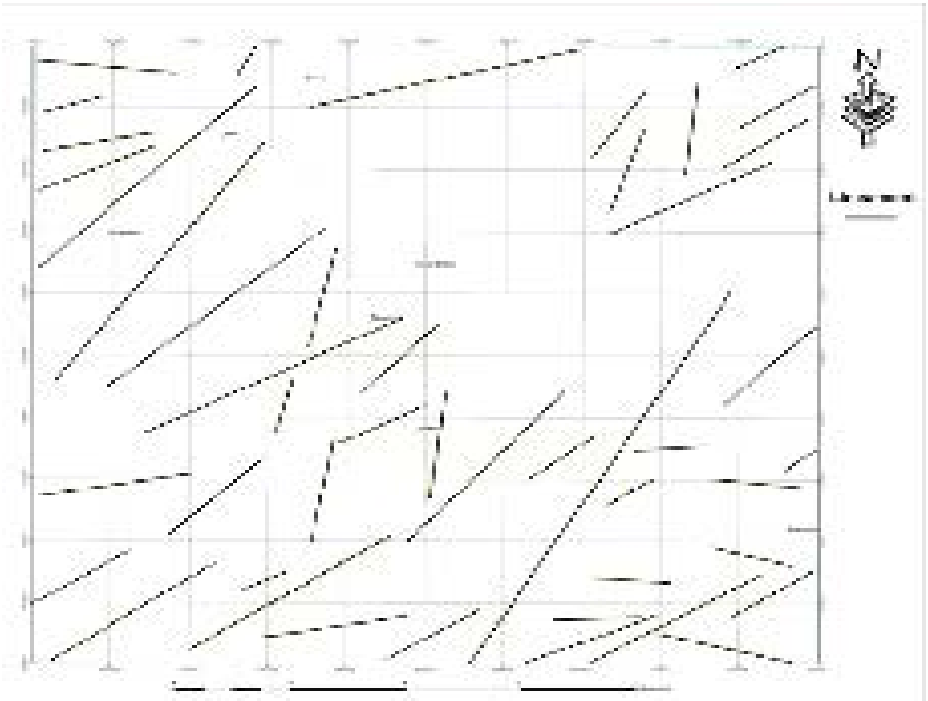

Figure 11: Lineament map produced from 1VD showing the lineaments been represented by the black lines.

part are oriented at angles between 020°-169°; 023°-118° the northwest; 020°-120° the southeast and 010°-120° the southwestern region of the study area. The density of these lineaments was observed to be highest towards the west than the eastern parts.

DEM was first acquired by downloading the satellite image from Shuttle Radar Topography Mission (SRTM). The DEM then imported to Erdas Imagine 9.2 to generate two forms of shaded reliefs, produced at 8 (0°, 45°, 90°, 135°, 180°, 225°, 270° and 315°) different angles at which the sun is inclined. Each shaded relief was made up of the combinations of several angles, though only two images were combined at a time which was used to generate the lineaments afterwards [33,34]. The two final images were saved and imported into PCI Geomatica where in each image (shaded relief), lineaments were

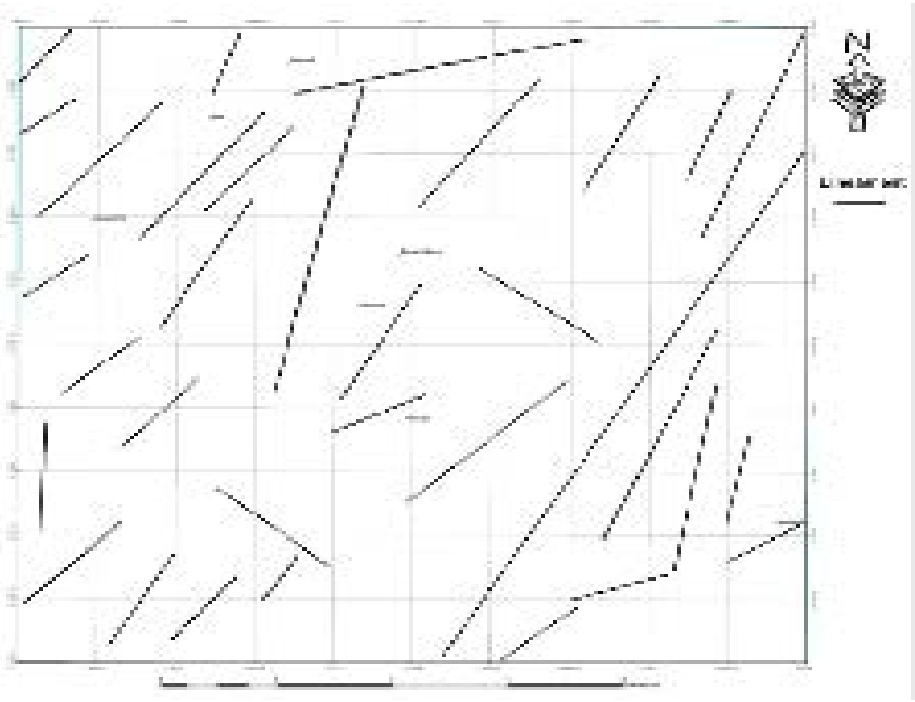

Figure 12: Lineament map generated from Analytical Signal.

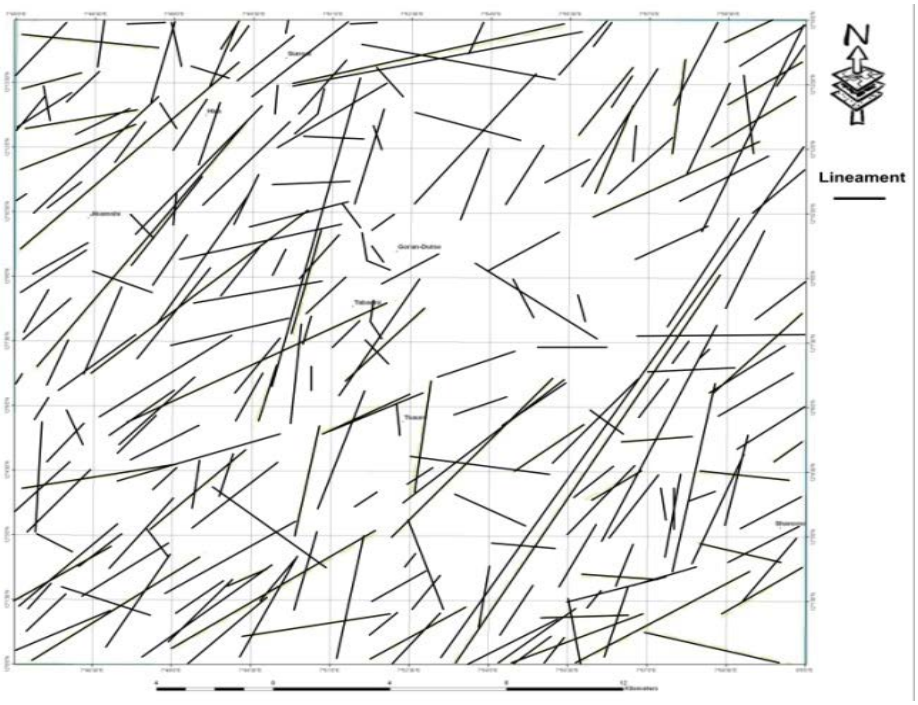

Figure 13: The study area showing all the lineaments extracted from satellite images and high resolution images.

generated separately. These images are exported as Arc Map shape files before been imported into Arc Map 9.3 software where the lineaments was digitized and lineament density map produced. Here, lineaments in each of the shaded relief image had buffers generated round them (buffer map). Both images were combined and areas of coincidences were displayed and the map underwent final digitization. There are two main contact zone caused by faulting in the study area. It can thus be inferred that both brittle and ductile deformation processes affected the area which led to shearing effects and series of fractures orienting majorly in a NE-SW direction (Figures 11-13).

Grey scale image of 1VD was generated to compliment the satellite images, in order to enhance and to show structural and lithologic details which were not in the satellite images (Figure 14). This

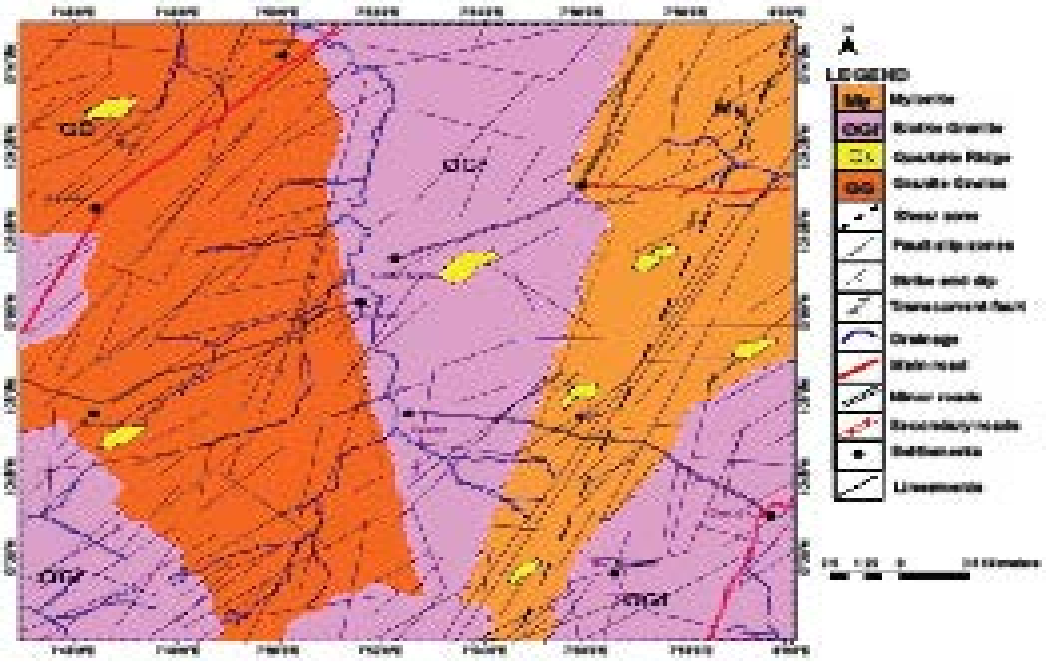

Figure 14: Structural map of the study area with lithologic units.

displays surface magnetic anomalies and/or local magnetic responses associated with geological structures. The grey areas were interpreted to have higher magnetic susceptibility while the black areas have low magnetic susceptibility. However, it also signifies that there are some earthly elemental substances such as sediments, mud, clay or water that decrease the magnetic susceptibility and hence, decrease the magnetic signal. It shows a major lineament trending NE-SW from southeast to northeast that can be traced towards the eastern parts of the study area.

These lineaments correspond to deep fractures, local faults, pegmatitic dykes/veins, ridges, river channels and furrows which are oriented E-W, NE-SW, NW-SE and have low magnetic susceptibility. It is observed at the lower part of the southeast quadrant that there may have been a truncation, perhaps a fault with a narrow displacement to the right (dextral). The areas with the higher magnetic signals due to its high susceptibility have values ranging from 0.6-1.1 nT and the areas with lower magnetic susceptibility have values between 0.0 and 0.5 nT.

The lineament map generated from 1VD showed few lineaments oriented NW-SE and the rest are in the NE-SW direction. The longest lineament which is interpreted as major fault is about 24 km towards the southeast whereas the shortest lineament runs less than 11 km in the southwest. The strike directions of these lineaments range between 008°-093° NE-SW. At the northwestern part of the study area, a possible dextral strike slip fault appears to be responsible for the displacement of two geological features, one to the right and the other to the left along the fault plane.

Analytical signal was derived from aeromagnetic data used to show areas with relative differences in electromagnetic properties. Analytical signal has an independent direction regardless of magnetization as its amplitude can however be related to the amplitude of magnetization [35]. An electromagnetic sensor sends infrared waves to land. Each geological feature has a radiation signature which is detected by the waves and recorded by an electromagnetic receiver which has been calibrated, with high signals reading between 0.1-0.3 nT and values from 0.1 nT are low. In other words, depends upon the amount of heat received and later reflected. However, the depth at which these signals were received and gathered to form datasets and then used to generate these images is absolute from less than 4 m. Three main electromagnetic anomalous zones were marked out with the highest zones represented by pink, intermediate zones by yellow and lowest zones by blue [36]. These zones also correspond to different lithologic units within the study area and zones of deformations especially fractures and faults can be carefully delineated. The areas with highest signals (pink and red) are dominated by granites, quartzite, mylonites and metasandstones. The areas with lowest signals (blue) are dominated by the gneisses. The greenish zones are dominated by part of the gneisses and the mylonites; orange and yellow areas by some medium-coarse grained granites and gneisses [37].

The structures are mostly oriented NE-SW with strike values ranging between 011°-077°, some are almost trending N-S but with a declination of about 003°. Few are oriented NW-SE with a strike of 130° and 125°. The longest lineament identified towards the southeastern part of the area is about 25.5 km with a strike of NE30°SW which is represented by discontinuous quartz ridge on field within the shear zone.

Satellite and aeromagnetic data correlation

The lineaments generated from the data sets were integrated to give a composite lineament map aimed at correlating the structural patterns and trends (Figures 14 and 15). Lineaments deduced were superimposed on the geological map and shows the rock types that have the most and least fractures (Figure 16). It was observed that the strike directions of the foliated rocks, the orientation of outcrops, stream channels, pegmatite dykes deep and shallow fractures, quartz ridges, shear and fault lines all corresponded to the deduced lineaments.

The study area was affected by both brittle and ductile deformational processes which led to the evolution of these structures. The fractures

are more towards the west than eastern part. It can be suggested that the minor fractures are subsidiaries of the major fractures that cuts through the study area (Figure 15). If there may be a future tectonic activity within the study area, these structures may further extend or expand and new ones may evolve because of the degree of fractures within the zone. The fractures also serve as routes through which water or hydrothermal solutions migrate and get trapped.

A graphical representation of the lineaments and their orientations was plotted. It shows that most of the lineaments trending NE-SW and NNE-SSW dominate the study area while the E-W lineaments are the least dominant. Aeromagnetic data (1VD and ASIG) generated fewer lineaments as compared to the satellite images (LANDSAT and DEM) that generated more lineaments (Figure 17).

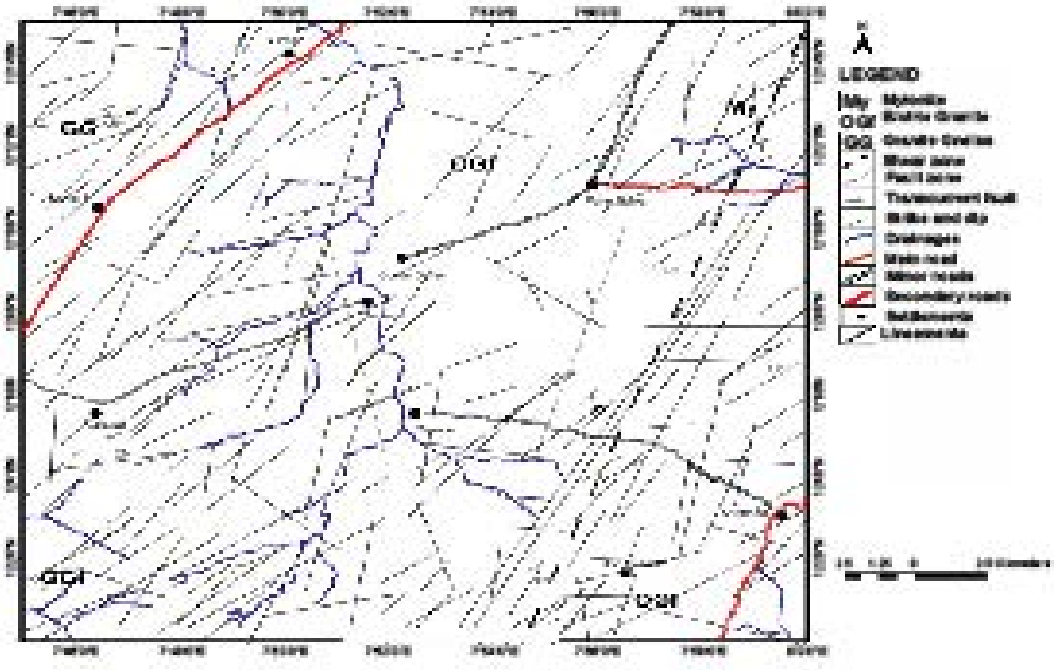

Figure 15: Structural map of study area which includes field, satellite and aeromagnetic data.

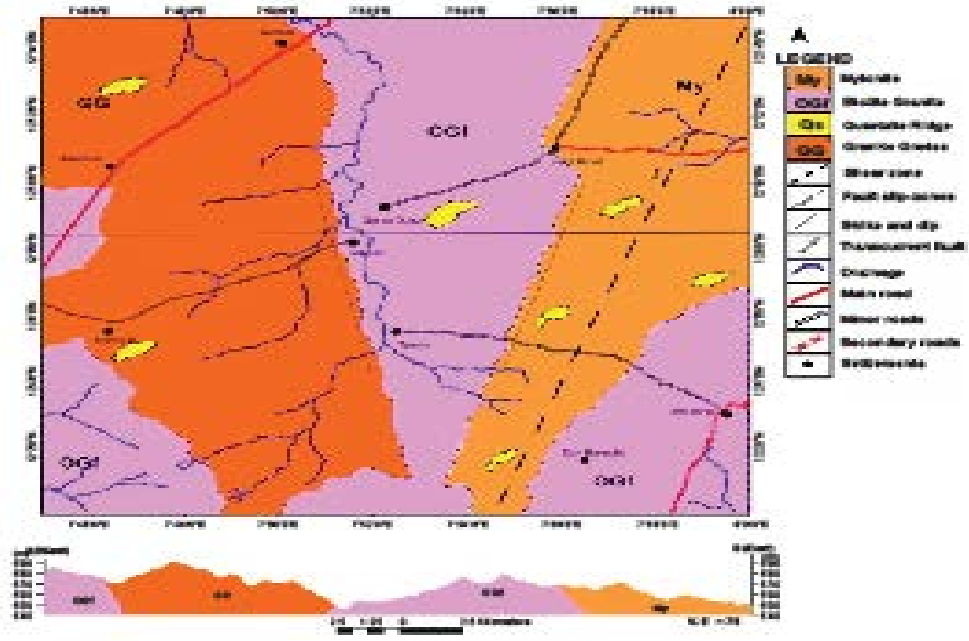

Figure 16: Geological map and cross section of the study area.

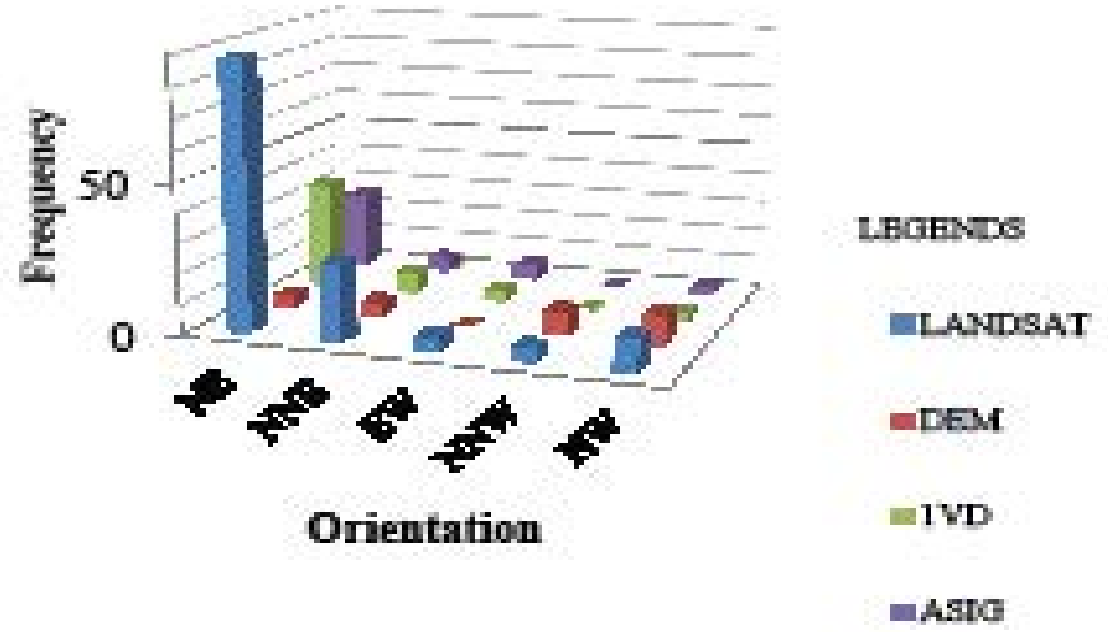

Figure 17: Statistical histogram of the lineaments.

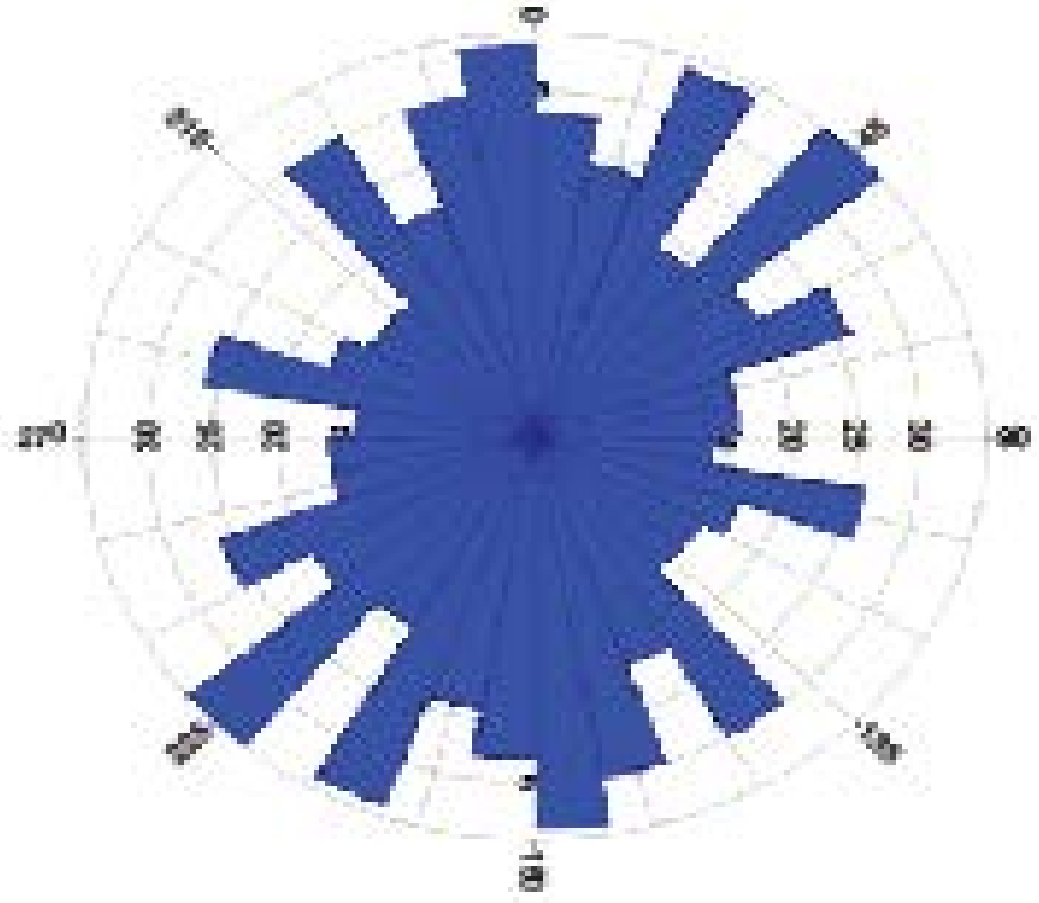

Figure 18: Rose diagram of all the joint readings from the study area.

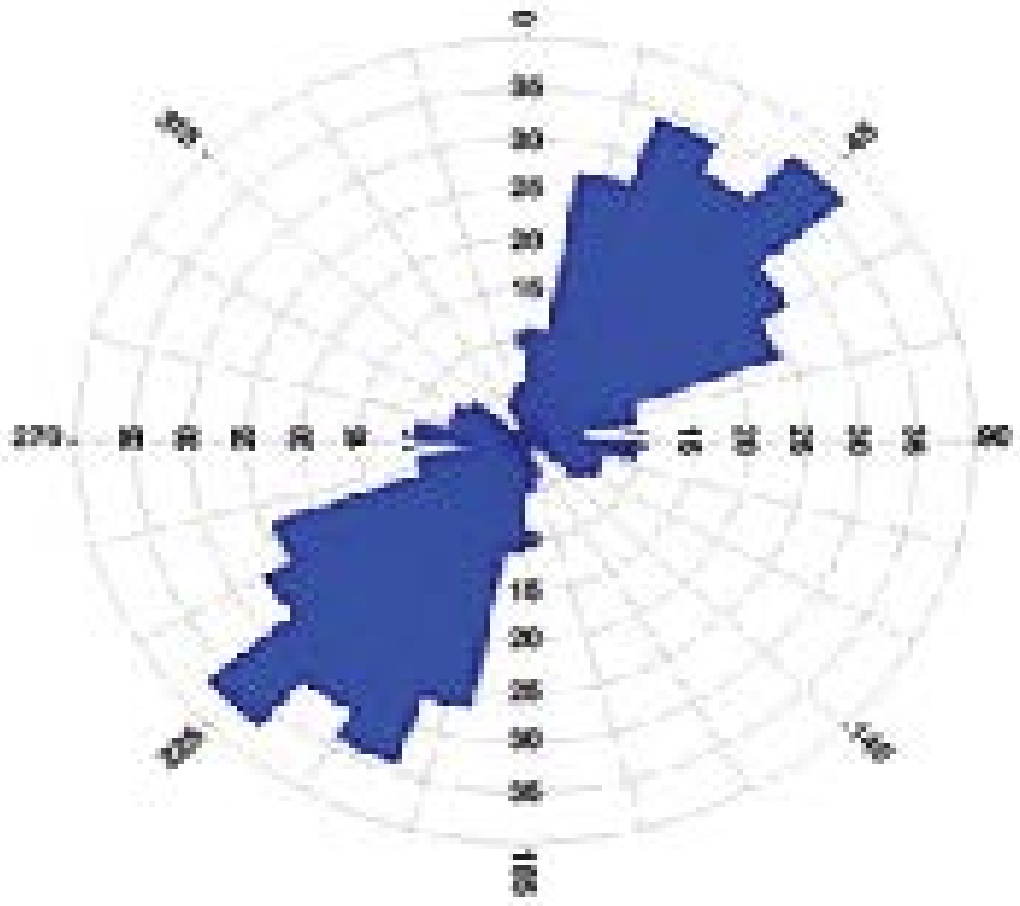

Figure 19: Rose plot of satellite and aeromagnetic lineaments combine.

Rose and stereo plots

Data obtained from field measurements of fractures, foliations and lineations were plotted on Rose Plots which shows NE-SW and NW-SE as the dominant trend directions (Figures 18 and 19). The NE-SW trending lineaments are associated with Pan-African Orogeny while the NW-SE trending lineaments are associated with Eburnean Orogeny [38]. Microstructures identified are sub grains around grain boundaries, micro foliations, elongated mineral grains within and around larger grains, bulging grain boundaries and deformation lamellae [39].

Conclusion

Multispectral and high resolution datasets have been successfully employed to have delineated shallow and near surface geological structures. Two fracture zones and lithologic boundaries were successfully marked out in the area. The Kalangai major fault cuts across the eastern part of the study area. It is deep seated and serves as migratory route for hydrothermal fluids as its being channeled to subsidiary fractures where they are trapped in veins, dykes and pegmatites. The lineaments been extracted correspond to series of discontinuous quartzite ridges, river channels and deep fractures in the study area. However, the cost of drilling, risk of inappropriate or drilling out of place can be reduced, areas prone to environmental hazards or source serving as exits of radioactive materials could be detected.

References

1. McCurry P (1976) The geology of the Precambrian Palaeozoic rocks of northern Nigeria- review. Geology of Nigeria 15-39.
2. Black R, Latouche L, Liegeois JP, Caby R, Bertrand JM (1994) Pan African displaced terranes in the Taureg shield (central Sahara). Geol 22: 641-644.
3. Caby R (1989) Precambrian terranes of Benin- Nigeria and northeast Brazil and the late Proterozoic South Atlantic fit. Geol Soc Am Spl Pap145-158.
4. Ajibade AC, Wright JB (1989) The Togo-Benin-Nigeria shield: Evidence of crustal aggregation in Pan-African belt. Tectonophys 165: 125-129 & 433-449.
5. Ball E (1980) An example of very consistent brittle deformation over a wide intercontinental area: The Late Pan-African fracture system of the Taureg and Nigerian shield. Tectonophysics 16: 363-379.
6. Wright JB, Hasting DA, and Williams HR (1985) Geology and mineral resources of West Africa: Allen and Unwin, London.187.
7. Grant NK (1970) Geochronology of Precambrian basement rocks from Ibadan, southwestern Nigeria. Earth Plan Sci Lett 10: 29-38.
8. Grant NK, Hickman M, Burkholder FR, Powell JL (1972) Kibaran metamorphic belt in the Pan-African domain of West Africa; Nature 134: 343-349.
9. Oversby VM (1975) Lead isotope study of aplites from the Precambrian rocks near Ibadan, Southwestern Nigeria. Earth Planetary Sci Let, 27: 177-180.
10. McCurry P, Wright JB (1977) Geochemistry and calc-alkaline volcanics in northwestern Nigeria, and a possible Pan-African suture zone. Earth Planet Sci Lett 37: 90-96.
11. Holt RW, Egbuniwe IG, Fitches WR, Wright JB (1978) The relationship between low grade metasedimentary belts, calc-alkaline volcanism and the Pan-African orogeny in northwestern Nigeria. Geol Rev 67: 631-646.

12. Oyawoye MO (1972) The basement complex of Nigeria. Geology Department, University of Ibadan, Nigeria. 67-99.

13. Obaje NG, Wehner H, Scheeder G, Abubakar MB, Jauro A, et al. (2004) Hydrocarbon prospective of Nigeria's inland basins: from the view point of organic petrology. Am Ass Petrol Geol Bull 87: 325-353.

14. Rahaman MA (1989) Review of the basement geology of south-western Nigerian. 2nd Edition of Geology of Nigeria, Rock View, Jos, Nigeria 39-56.

15. Truswell JF, Cope RN (1963) The geology of parts of Niger and Zaria provinces, northern Nigeria. Bull Geol Sur Nigeria 29.

16. McCurry P (1970) The geology of degree sheet 21, Zaria, Nigeria. Unpublished M.Sc. thesis,Ahmadu Bello University, Zaria.

17. Akinyede OA (1981) A geochemical stream sediment survey in Kafur-Malumfashi area, Kaduna State, Nigeria. Unpublished M.Sc. Thesis, Ahmadu Bello University, Zaria.

18. Higgins M (1971) Cataclastic Rocks. Professional paper, USA Geological Survey,97.

19. Sibson RH. (1967) Fault rocks and fault mechanisms. J Geol Soc Lon 133: 191-214.

20. Mower CK (1986) What is a mylonite? Geoscience Canada 13.

21. Danbatta UA (2003) The lithogeochemical framework underlying the geotectonic evolution of the Kazaure Schist belt, northwestern Nigeria. The Nig J Sci Res 4: 1-13.

22. Abubakar YI (2012) An integrated technique in delineating structures: Case study of Kushaka schist belt, northwestern Nigeria. Int J App Sci & Technol 5: 164-173.

23. Turner DC, Webb PK (1974) The Daura igneous complex, northern Nigeria, a link between the Younger Granite districts of Nigeria and southern Niger. J Geol Soc Lon 133: 71-77.

24. Grant NK (1978) Structural distinction between a metasedimentary cover and an underlying basement in the 600 m.y old Pan-African domain of northwestern Nigeria, West Africa. Geol Soc Am Bull 89: 50-58.

25. Ajibade AC, Fitches WR, Wright JB (1979) The Zungeru mylonites, Nigeria: Recognition of a major tectonic unit. Rev Dyn Geol & Phy Geog 21: 359-363.

26. McCurry P (1973) Geology of degree sheet 21, Zaria, Nigeria. Overseas Geol & Min Res 45.

27. McCurry P (1978) Geology of degree sheet 10 (Zuru), 20 (Chafe), and part of 9(Katsina), Nigeria. Overseas Geology of Mining Resources, 53 H.M.S.O. London.

28. Danbatta UA, Ike EC (2001) Geochemistry and origin of metasediments from the Kazaure Schist belt in the Precambrian basement of northwestern Nigeria. Nig J Chem Res 6: 31-36.

29. Danbatta UA, Garba I (2007) Geochemistry and petrogenesis of Precambrian amphibolites in the Zuru Schist belt, northwestern Nigeria. J Min & Geosci Soc 43: 23-30.

30. Waziri NM (2012) Environmental geochemistry of Soils and Stream Sediments from the Anka and Birnin-Gwari Artisanal Gold Mining areas, NW Nigeria. Unpublished PhD Thesis, University of East Anglia UK.

31. Waziri NM (2014) Environmental geochemistry of Soils and Stream Sediments from the Birnin Gwari Artisanal Gold Mining Area, Northwestern Nigeria. Univ J Geosci 2: 18-27.

32. Russ W (1957) The geology of parts of Niger, Zaria and Sokoto provinces, with special reference to the occurrence of gold. Bull Geol Sur Nigeria 27.

33. Abdullah A, Akhir JM, Abdullah I (2010) The extraction of lineaments using slope image derived from digital elevation model: case study: Sungai Lembing-Maran area, Malaysia. J App Sci Res 6: 1745-1751.

34. Andongma WT (2014) Geology, remote sensing and geochemistry of sheet 52 NE (Anka), Northwestern Nigeria. An Unpublished M.Sc. Thesis, Ahmadu Bello University, Zaria.

35. Silva AM, Pires AC, McCafferty A, Moraes R, Xia H, et al. (2003) Applicationof airborne geophysical data to mineral exploration in the uneven exposed terrains of the Rio Das Velhas greenstone belt. Journal of Geosciences 33: 17-28.

36. Asadi HH, Hale M (1999) Integrated analysis of aeromagnetic, Landsat TM and mineral occurrence data for epithermal gold exploration in northwest Iran, 13th Intern Conf on App Geol Rem Sens 8.

37. Danbatta UA (1999) Geotectonic evolution of the Kazaure schist belt of northwestern Nigeria. Unpublished Ph.D. Thesis, Ahmadu Bello University, Zaria.

38. Ekwueme BN (1983) Regional metamorphism of pelitic rocks SE Lokoja. Nige J Min & Geol Sci 20: 17-24.

39. Garba I (2003) Geochemical characteristics of mesothermal gold Mineralization in the Pan African (600 + 150 ma) basement of Nigeria. App Earth Sci 36: 123–135.